IMPROVED DYNAMIC STRAIN HARDENING IN POLY(URETHANE UREA) ELASTOMERS FOR TRANSPARENT ARMOR APPLICATIONS

Alex J. Hsieh*
U.S. Army Research Laboratory
AMSRD-ARL-WM-MD
Aberdeen Proving Ground, MD 21005-5069

Sai S. Sarva
Institute for Soldier Nanotechnologies
Massachusetts Institute of Technology
Cambridge, MA 02139

Norman Rice
Triton Systems, Inc.
Chelmsford, MA 01824

ABSTRACT

The U.S. Army Joint Service Chemical/Biological Protective Facemask program requires a lens system that can be folded while providing a high level of optical quality, chemical resistance, ballistic protection, scratch resistance, and environmental durability. In general, materials with good barrier properties lack significant energy absorption/dissipation abilities upon impact, whereas rigid transparent polymeric materials that are extremely tough exhibit poor resistance to chemical hazards and abrasion. The Army Research Laboratory is currently engaged in collaboration with the Institute for Soldier Nanotechnologies (ISN) to help design novel polymeric materials with improved physical and mechanical properties by exploiting novel molecular mechanisms. This paper presents recent experimental findings exploring the role of molecular mechanisms on the dynamic mechanical deformation of a model set of transparent segmented poly(urethane urea), PUU, elastomers. As expected, increasing the hard segment content improved the barrier properties, and also increased the stiffness and flow stress levels. Tailoring of the microstructure was critical in altering their rate-dependent mechanical behavior. It was observed that promoting phase mixing among the hard and soft segment domains of the microphase-separated PUU material greatly enhanced its rate-dependent stiffening and strain hardening behavior. Furthermore, the resulting increase in intermolecular interaction also enhanced the barrier properties. These insights can aid in the design of PUUs for articles that manifest improved protective abilities under impact, while maintaining their flexibility during normal use, which is greatly desired for chemical/biological protective faceshield applications.

1. INTRODUCTION

Segmented poly[urethane urea] (PUU) elastomers, like polyurethane (PU) based materials, exhibit versatile physical and mechanical properties. Additionally, PUU materials are unique, especially due to their capabilities to be processed into fibers, coatings as well as transparent flexible or rigid articles. The performance requirements for various platforms can be significantly different. Transparent, reaction-cast PUUs have very good barrier properties against chemical and UV degradation, and are being used to replace polycarbonate as a lens material in the current U.S. Army Joint Service General Purpose Mask (JSGPM) program. Yet, some of the PUUs capable of ballistic protection exhibited a profound compromise in fold recovery [Grove, 1999]. Complete and rapid fold recovery capability is very important for face mask protective systems that are designed for use in first response and special force operations, especially after extended periods of being folded in storage. In general, high elasticity and toughness are greatly desirable. While high stiffness is critical to help defeat the threat, resilience and toughness are essential for energy absorption and dissipation. To optimize the performance of PUUs, it is necessary to gain a better understanding of micro-mechanisms that govern the mechanical behavior over a range of low to very high strain rates.

The chemical structure of a PUU generally consists of long-chain polyols and diisocyanates connected with short-chain diamines, which are used as chain extenders. The long-chain polyols and diisocyanates form soft segments with urethane linkages, whereas the short chain diamines react with diisocyanates to form hard segments with urea linkages. Microphase separation resulting from the thermodynamic incompatibility between the hard and

Report Documentation Page

Form Approved
OMB No. 0704-0188

1. REPORT DATE	2. REPORT TYPE	3. DATES COVERED
DEC 2008	**N/A**	**-**

4. TITLE AND SUBTITLE	5a. CONTRACT NUMBER
Improved Dynamic Strain Hardening In Poly(Urethane Urea) Elastomers For Transparent Armor Applications	5b. GRANT NUMBER
	5c. PROGRAM ELEMENT NUMBER
6. AUTHOR(S)	5d. PROJECT NUMBER
	5e. TASK NUMBER
	5f. WORK UNIT NUMBER
7. PERFORMING ORGANIZATION NAME(S) AND ADDRESS(ES) **U.S. Army Research Laboratory AMSRD-ARL-WM-MD Aberdeen Proving Ground, MD 21005-5069**	8. PERFORMING ORGANIZATION REPORT NUMBER
9. SPONSORING/MONITORING AGENCY NAME(S) AND ADDRESS(ES)	10. SPONSOR/MONITOR'S ACRONYM(S)
	11. SPONSOR/MONITOR'S REPORT NUMBER(S)

12. DISTRIBUTION/AVAILABILITY STATEMENT
Approved for public release, distribution unlimited

13. SUPPLEMENTARY NOTES
See also ADM002187. Proceedings of the Army Science Conference (26th) Held in Orlando, Florida on 1-4 December 2008, The original document contains color images.

14. ABSTRACT

15. SUBJECT TERMS

16. SECURITY CLASSIFICATION OF:			17. LIMITATION OF ABSTRACT	18. NUMBER OF PAGES	19a. NAME OF RESPONSIBLE PERSON
a. REPORT	b. ABSTRACT	c. THIS PAGE			
unclassified	**unclassified**	**unclassified**	**UU**	**8**	

soft segments gives rise to a broad range of physical and mechanical properties [Holden et al., 1996]. The choice of diisocyanates, long chain polyols and chain extenders greatly affects the ability of the soft and hard segments to crystallize, as well as to microphase separate, and hence is crucial to tailoring the microstructure and the resulting macroscopic properties of these elastomers.

Previously, studies have been conducted to examine the mechanical deformation of PUs and PUUs [Sheth et al., 2004; Qi and Boyce, 2005; James Korley et al., 2006; Yi et al., 2006; Sarva et al., 2007]. Sheth et al. systematically evaluated the influence of soft segment (SS) molecular weight, hard segment (HS) content and the chain extender type on the dynamic mechanical behavior of 4,4′-dicyclohexylmethane diisocyanate (HMDI)-polydimethylsiloxane (PDMS) based PUs and PUUs [Sheth et al., 2004]. Their results showed that the molecular weight of PDMS and the length and symmetry of the chain extenders (diols for urethanes and diamines for ureas) had a marked effect on the morphology, the rubbery plateau modulus and the tensile behavior of both PU and PUU materials. Generally, it was observed that the degree of microphase separation and the values of rubbery plateau and tensile modulus were significantly greater in the PUU than in the corresponding PU. This was attributed to a difference in the cohesive strengths of the bidentate in urea versus the monodentate in urethane. The overall rate-dependent mechanical behaviors of PUs and polyureas have also been studied. Qi and Boyce examined the compressive stress-strain behavior, including the nonlinear hyper-elastic behavior, time dependence, hysteresis, and softening of a segmented PU [Qi and Boyce, 2005]. They also developed a physically-based constitutive model to capture various features of the mechanical behavior; an excellent agreement between the experimental results and the model predictions was demonstrated. Boyce and co-workers have also examined the high strain-rate compressive behavior of PUs and a polyurea [Yi et al., 2006; Sarva et al., 2007]. As the strain rate was increased, the stress-strain behaviors were observed to transition from a rubbery type behavior to a leathery or a glassy type behavior. These transitions in the stress-strain behavior were directly associated with the corresponding rate-dependent viscoelastic behavior shifts observed through dynamic mechanical analysis. Their studies of PUs indicated that incorporation of dimethyl propanediol (DMPD) as a chain extender resulted in greater strain-rate sensitivity in comparison to the incorporation of butanediol (BDO); as the strain rate was increased from 10^{-3} – 10^{4} s^{-1}, the initially rubbery DMPD-containing PU transitioned to a distinctly glassy type behavior. The DMPD-containing PU, however, exhibited a large compromise in fold recovery, unlike the PU with BDO, which was able to unfold rapidly and completely after being released from bending [Hsieh et al., 2006].

Results of our recent studies have revealed that promoting phase mixing via increased intermolecular interaction between the hard and soft segments is much more effective than simply increasing the hard segment contents to improve barrier properties of select model PUs and PUUs against chloethyl ethyl sulfide, a simulant for the Chemical Warfare blister agent, HD [Hsieh et al., 2008]. The objective of the ongoing research is to gain a better understanding of the molecular mechanisms that govern both the mechanical and permeation behavior of segmented PUUs. In particular, understanding the very high strain rate mechanical behavior is critical for the design of segmented PUs and PUUs. In this work we examine a set of model PUU materials and aim to elucidate the effects of composition, including the HS content and the molecular weight of the PTMO soft segment on the morphology, viscoelastic behavior and the rate-dependent mechanical behavior. Results obtained through characterization techniques, including small-angle X-ray scattering (SAXS), differential scanning calorimetry (DSC), and dynamic mechanical analysis (DMA) are used to correlate with and analyze the stress-strain data of these PUUs over a broad range of strain rates.

2. EXPERIMENTAL

2.1 Materials

In this study, we have synthesized a set of model PUU materials by following a two-step, pre-polymer synthesis method from 4,4′-dicyclohexylmethane diisocyanate (HMDI - Desmodur W, Bayer MaterialScience), poly(tetramethylene oxide) (PTMO - PolyTHF, BASF Corporation), and a chain extender, diethyltoulenediamine (DETA - Ethacure® 100-LC, Albemarle Corporation, Baton Rouge, Louisiana). Table 1 lists the compositions of the four different PUU materials chosen for evaluation. PUU A is the baseline material, whereas PUU B and PUU C are materials in which the hard segment (HS) content has been successively increased. In PUU D, the chemical molar composition is similar to PUU A, but the molecular weight, MW, of the soft segment (SS), poly(tetramethylene oxide), is varied from 2000 to 1000 g/mol. The HS contents (%HS) noted in Table 1 were calculated using an approach based on the urea content, as described by the below equation [O'Sickey et al., 2002]:

$$\%HS = \frac{100\,(R-1)(M_{di}+M_{da})}{(M_g+R(M_{di})+(R-1)(M_{da}))} \qquad (a)$$

where R is the molar ratio of the diisocyanate to PTMO, and M_{di}, M_{da} and M_g are the number average molecular weights of the diisocyanate, diamine and PTMO, respectively [O'Sickey et al., 2002]. The experimental

results described in the following sections will be examined in correlation with the HS content values noted here.

Table 1. The molecular weight of PTMO and the HS contents of the synthesized PUU materials

	MW of PTMO (g/mol)	Hard Segment Content (wt%)
PUU **A**	2,000	16.3
PUU **B**	2,000	28.0
PUU **C**	2,000	36.9
PUU **D**	1,000	25.9

2.2 Characterization

SAXS measurements were performed using CuKα radiation (λ = 1.5418 Å) generated from a Rigaku rotating anode source operated at 40 kV/60 mA, and monochromated by a pyrolytic graphite crystal. Data were collected using a Molecular Metrology 2D multi-wire area detector placed ~65 cm from the sample. The data were azimuthally averaged and corrected for air scatter and detector anomalies. The location of the scattering maximum corresponds to the average periodic spatial resolution between the microdomains, and the average interdomain spacing, d, is estimated using the Bragg's law as:

$$q = 4\pi \sin\theta/\lambda = 2\pi d \qquad (b)$$

where q is the scattering vector, λ is the wavelength of the incident radiation and θ is one half the scattering angle.

Dynamic mechanical analysis (DMA) measurements were carried out using a TA Instruments Q800 DMA in tension mode. Rectangular specimens with dimensions of 3 mm width, 2 mm thickness and 12 mm gauge length were used. Tests were conducted at frequencies of 1, 10 and 50 Hz, using a constant strain amplitude of 0.1%, for a temperature range of -150 to 200 °C at a ramp rate of 3 °C/min. Quasi-static mechanical testing was performed under uniaxial compression at low strain rates using a Zwick screw-driven mechanical tester. These tests were performed at strain rates ranging from 10^{-3} to 10^{-1} /s, under conditions of constant nominal strain rate. The samples were also unloaded at the same strain rate to examine the recovery of the elastic deformation and gauge the permanent set deformation. A single set of uniaxial tension tests was performed at a strain rate of 10^{-3}/s to compare against the compressive tests. High strain rate tests were also conducted under uniaxial compression at high strain rates in the range of 10^{3} – 10^{4} /s, using a split Hopkinson pressure bar (SHPB) at the MIT Institute for Soldier Nanotechnologies (ISN). The bars were made of aluminum, and the incident and transmission bar were each of 19.75 mm diameter and 2.9 m length; the striker bar was of 51 cm length. A range in strain rates was accomplished by varying the striker bar impact velocity. The complete details of SHPB testing procedures for polymeric materials can be found in [Gray et al., 2000; Chen et al., 2002].

3. RESULTS AND DISCUSSION

3.1 Microstructures via Small-Angle X-ray Scattering (SAXS)

Figure 1 compares the scattering intensities for the four materials, exhibiting the effects of varying the HS content and the SS molecular weight (MW). The base material, PUU **A**, exhibits a broad scattering peak with an average interdomain spacing of ~15.9 nm, suggesting the presence of isolated HS domains as is typically observed in microphase-separated PUUs. For the series of PUU 2k samples (i.e. with the PTMO MW being maintained the same), the intensity of the scattering peak successively increases when the PUU **A**, **B** and **C** materials are compared. This can be attributed to the increase in scattering contrast between the HS domains and the SS regions, with increasing HS content. In comparison to the PUU **A**, the scattering peak of the PUU **B** is observed to shift to a smaller angle, indicating an increase in the average interdomain spacing to ~28.8 nm due to a growth in the HS domain size. As the HS content is further increased, the scattering peak for the PUU **C** grows in intensity, but becomes relatively broad and indistinct. This lack of a pronounced scattering peak at high HS contents, as previously observed by Abouzahr et al., could result either from an emergence of growingly irregular shape of the HS domains or from an onset of a significant change in the morphology, such as an increased interconnectivity of HS domains [Abouzahr et al., 1982].

The scattering characteristics also differ when the molecular weight of the soft segment is varied. Figure 1 shows that the scattering peak for the PUU **D** material is located at a comparatively large angle and exhibits a significantly decreased intensity. The peak location for the PUU **D** corresponds to an average interdomain spacing of ~11.4 nm. Keeping the molar ratio the same, a reduction in the SS molecular weight from 2000 g/mol to 1000 g/mol results in a smaller SS content, which contributes to the decrease in the HS interdomain spacing. Note that the HS interdomain spacing for the PUU **D** is significantly smaller than the PUU **B**, even though both have similar HS/SS contents. The SS content remaining the same, the molar content of the SS hydroxyl groups in the PUU **D** is twice that of the PUU **B**. Hence a greater number of isocyanate groups are consumed through reactions with the greater number of SS diols in the PUU

D, causing a fewer number of isocyanate groups being available to react with the diamines to form urea linkages due to stoichiometric requirements. This leads to a smaller HS domain size and a much smaller HS interdomain spacing in the PUU **D**.

Additionally, the scattering peak for the PUU **D** exhibits a significantly reduced intensity indicating a lowered X-ray contrast. The molar content of the urethane linkages connecting the soft segments within the SS domains in the PUU **D** is approximately twice that in the PUU **B** since the former has twice the molar content of the SS hydroxyl groups. This leads to an increase in the intermolecular interactions, via hydrogen bonds between the hard and the soft segments, and a greater phase mixing.

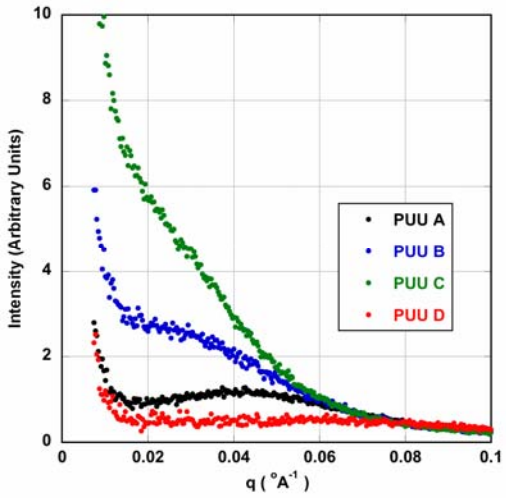

Figure 1. SAXS data for the various samples

3.2 Dynamic Mechanical Analysis (DMA) Measurements

Effect on the storage modulus - Figure 2 shows the storage moduli curves for the PUU materials at 1Hz frequency. The curve for the base material, PUU **A**, shows that when the soft segment glass transition temperature, $T_{g,s}$, is surpassed at -64 °C, the onset of SS mobility results in a very drastic decline in the modulus (a drop of over two orders of magnitude) until the rubbery plateau is eventually reached. The storage moduli curves for the PUU 2k materials show a considerable increase in the rubbery plateau modulus with increasing HS content. To quantify this effect, the magnitudes of the rubbery plateau moduli were determined at a temperature of 75 °C; these are listed in Table 2 and also shown in the inset of Figure 2. A very strong dependence of the rubbery plateau modulus on the HS content is observed. The modulus rises from 12 MPa for the PUU **A** with a 16.3% HS content to 260 MPa for the PUU **C** material with a 36.9% HS content. Similar strong, non-linear dependence of the elastic modulus on the HS content was also observed by Abouzahr et al. in their studies of stress-strain behavior of PUs. They attribute this to morphological changes that arise at high HS contents, such as the interlocking of the HS domains [Abouzahr et al., 1982].

Additionally, the SS molecular weight significantly alters the nature of the storage modulus curve. In comparison to the PUU **B**, the PUU **D** material exhibits a significant difference in its curve (note again that though PUU **A** was the base formulation for the 2k materials, when comparing the effect of the SS molecular weight, we compare the properties of the PUU **B** with the PUU **D** due to their similar HS contents). At 75 °C, the rubbery plateau modulus for the PUU **D** is lower, but as the temperature is decreased, its storage modulus rises at a faster rate and at ~5 °C, it crosses over with the PUU **B** material. By -50 °C, the PUU **D** has a significantly greater modulus than the PUU **B**. This change in shape of the storage modulus curve is caused by the shifting of the soft segment glass transition temperature and the hard segment glass transition temperature towards each other seen in the differential scanning calorimetry data (not shown) for the PUU **D** material, which is a result of the greater phase mixing in this material. In polymers, there exists a time-temperature equivalence in their viscoelastic behavior [Ferry, 1980], and hence lowering the temperature is equivalent to increasing the strain rate. These storage moduli curves demonstrate that though the PUU **D** material is more compliant than the PUU **B** at lower strain rates (higher temperatures), it will be significantly stiffer than the PUU **B** at higher strain rates (lower temperatures).

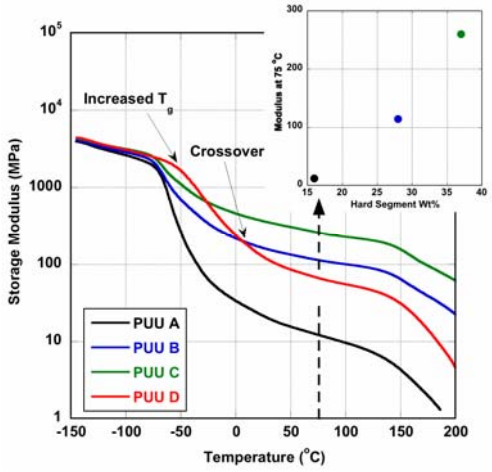

Figure 2. DMA storage moduli curves at 1 Hz for the various PUU materials. Inset shows the effect of HS content on the rubbery plateau modulus at 75 °C

Table 2. The values of rubbery plateau modulus, E′, determined at 75 °C

	E′ at 75 °C (MPa)
PUU **A**	12
PUU **B**	114
PUU **C**	260
PUU **D**	67

Effect on the soft-segment glass transition - The precise $T_{g,s}$ locations for the PUU materials were determined from the DMA loss modulus data; see Table 3. For the PUU 2k samples, the change in the HS content did not exhibit any significant effect on the $T_{g,s}$ location. However, the increase in the HS content was accompanied by a substantial decrease in the loss factor (tanδ) intensity. Figure 3 shows the tanδ curves obtained at a frequency of 1 Hz for the PUU 2k samples. As the HS content is increased, the number of physical crosslinks that are available to restrict the SS chain mobility also increases and hence the tanδ intensity, which characterizes the damping behavior, successively decreases. For the PUU **C** material, the intensity is almost one half the intensity for the PUU **A** material, indicating a greatly reduced damping behavior. These materials exhibit multiple relaxation peaks, associated with the $T_{g,s}$ in the -75°C and 50°C range. The PUU **A** material exhibits a very distinct and intense peak at -64°C along with a much less intense shoulder at 21°C. The more intense and dominant peak relates to the relaxation of the SS rich phase and the less dominant shoulder presumably relates to the SS and HS phase mixed regions [Kojio et al., 2007]. As the HS content is increased, the dominant tanδ peak becomes less distinct. Also, two separate peaks are seen to emerge from the dominant peak for the PUU **B** and PUU **C** materials. Further characterization of these multiple SS relaxation peaks is currently in progress.

Variation in the SS molecular weight also has a great effect on the $T_{g,s}$. The $T_{g,s}$ for the PUU **D** is ~ 20 °C higher than that for the PUU 2k materials (see Figure 3 and Table 3); note that this increase in $T_{g,s}$ for the PUU **D** was also observed in the DSC data (not shown). Also, the natures of the tanδ peaks for the 2k materials and the PUU **D** material are vastly different. The PUU **D** displays a single broad tanδ peak, which appears to be a result of the merging of the multiple SS relaxation peaks that were observed in the 2k materials. This is likely due to a change in morphology as a result of the greater phase mixing in the PUU **D** material.

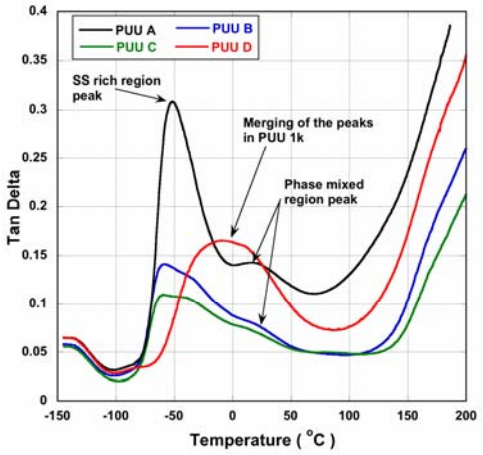

Figure 3. Plots of tanδ as a function of temperature for the four materials

Effect on the rate dependency: Recently, it has been demonstrated that the rate-sensitive mechanical behavior of polymeric materials is directly associated with the rate/frequency dependent shifts in their viscoelastic behavior [Yi et al., 2006; Mulliken and Boyce, 2006; Sarva et al., 2007]. In order to compare the rate sensitive behaviors of these PUUs, the DMA measurements were extended to determine the frequency dependent shifts in their viscoelatic behaviors. Figure 4 shows the storage modulus curves for the PUU **B** and the PUU **D** materials, which have comparable HS contents, at 1 and 50 Hz frequencies. The increase in frequency results in the storage modulus curves shifting to the right causing an increase in modulus at any given temperature. This increase in modulus is governed by the rate at which the various viscoelastic transitions shift and the evolving shape of the storage modulus curve with increasing rate/frequency. The shift in $T_{g,s}$ is of particular importance here since it primarily governs the room temperature mechanical behavior due to its proximity. Figure 4 also shows the loss modulus peaks of the $T_{g,s}$ for the two materials at the two frequencies. The $T_{g,s}$ for the PUU **D** clearly demonstrates a greater shift (~11°C) than the PUU **B** (~7°C), indicating a lower activation energy for the 1k material. Table 3 lists the $T_{g,s}$ values (determined from the DMA loss modulus data) at frequencies of 1 Hz, 10 Hz and 50 Hz for all the materials. These frequencies are equivalent to loading the materials at strain rates[1] of ~ 4×10^{-3}, 4×10^{-2} and 4×10^{-1}/s, respectively. On an average, the $T_{g,s}$ for the PUU 2k samples shifts by ~4 °C per

[1] Following Mulliken and Boyce, the strain rate is estimated from the test frequency using the relation:

$$\text{strain rate} = \frac{\text{strain}}{\text{time}} = \frac{d_0 / L_g}{\omega / 4},$$

where d_0 is the displacement amplitude, L_g is the specimen gauge length and ω is the test frequency [Mulliken and Boyce, 2006].

decade of strain rate, and is nearly the same for all of them. But for the PUU 1k material, the shift is nearly 7-8 °C per decade of strain rate, almost twice that of the 2k materials. These rates of shift correspond to apparent activation energies of ~203 kJ/mol and ~161 kJ/mol for the 2k and 1k materials, respectively. Hence, at a given temperature, increasing the strain rate by a certain amount will result in a comparatively greater increase in the 1k material modulus compared with that of the 2k material. This in addition to the steeper rise in the modulus for the PUU **D**, due to the shape of its storage modulus curve (see Figure 2) predicts that the PUU **D** material will exhibit a substantially greater rate-dependent stiffening than the 2k material due to the greater phase mixing and increased intermolecular interactions.

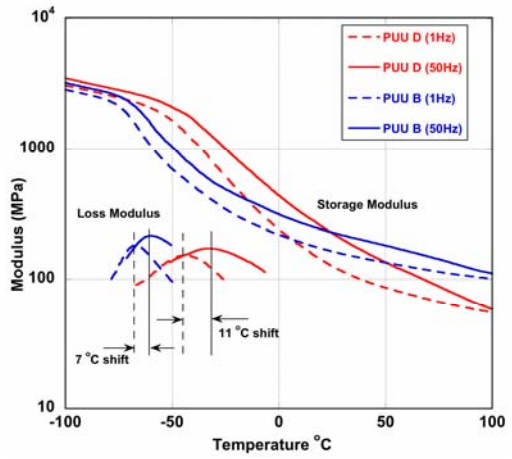

Figure 4. DMA curves at 1 Hz and 50 Hz for the PUU **B** and PUU **D**

Table 3. Values of $T_{g,s}$ determined from DMA for the PUU samples

	$T_{g,s}$ (°C) obtained using DMA loss modulus data at a frequency of		
	1Hz	10Hz	50Hz
PUU **A**	-64	-60	-58
PUU **B**	-67	-62	-60
PUU **C**	-67	-64	-59
PUU **D**	-44	-37	-33

3.3 Rate-Dependent Stress-Strain Behavior

To confirm the predictions of the DMA results, the stress-strain behaviors of these PUUs were examined over a range of low and high strain rates.

Stress-strain behavior under uniaxial compression – The stress-strain behavior for the four materials over the entire range of strain rates (10^{-3} – 10^{4} /s) are highly nonlinear and rate dependent. The curves are initially linear and relatively stiff followed by rollover to a more compliant behavior. With increasing strain, the stress levels increase as the curves exhibit strain hardening due to increasing orientation of the polymer chains at large strains. Additionally, the stress levels also increase with increasing strain rate. For a more precise comparison of the nature of the stress-strain curves, the curves for the four materials at a low strain rate (10^{-3} /s) and a high strain rate (~4500 /s) are shown in Figure 6. The low rate curves in Figure 6A clearly show the magnitude of increase in the stress levels with the increase in HS content in the PUU 2k materials. It is interesting to note that the inelastic strain following recovery (permanent set deformation) successively increases with the HS content. PUU **C** exhibits the greatest permanent set deformation. This is presumably due to an irreversible disruption of the interconnected HS domains, as previously suggested by Abouzahr et al. [Abouzahr et al., 1982]. Figures 6A and B also show the stress-strain curves for the PUU **D**. At a low strain rate, in comparison to the PUU **B**, the PUU **D** has much lower stress levels. But at high strain rate (see Figure 6B) the stress levels for the PUU **D** are visibly higher. This confirms the trend observed in the DMA data which predicted a significantly greater rate-depending stiffening for the PUU **D** due to its microstructure with greater phase mixing. To accurately gauge the trends in rate sensitivity, the flow stress values for the PUU materials are plotted against strain rate on a logarithmic scale in Figure 7; the flow stress values in the figure are those attained at 0.3 true strain[2]. At high rates, the flow stress values exhibit a marked increase. The comparatively greater strain-rate sensitivity for the PUU **D** is evident. In the low rate range, the flow stress values for the PUU **D** are lower than the PUU **B** by ~2 MPa, but at high rates they are higher by ~5 MPa. This behavior exhibited by the PUU **D**, where it is more compliant under static loading conditions, but exhibits greater strengthening at high rates, is highly desirable for a range of impact resistant applications. Such properties can help provide rapid and complete unfolding capabilities that are critical during normal use for articles such as face-masks and concurrently provide improved protection under impact.

[2] At this strain level, the stress-strain curves have rolled over to flow and are devoid of any significant strain hardening effects. Also dynamic equilibrium has been achieved for the high rate tests at this strain [Sarva et al., 2007]

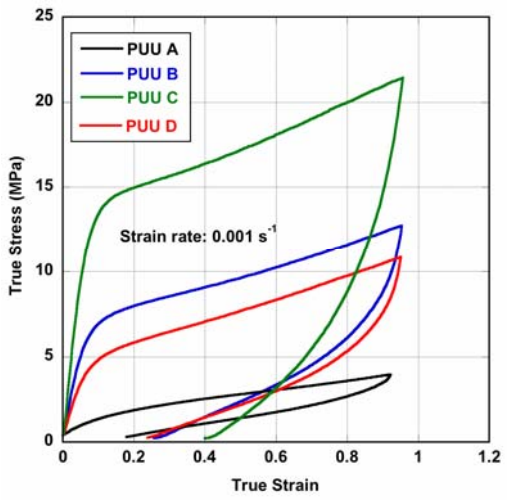

(6A)

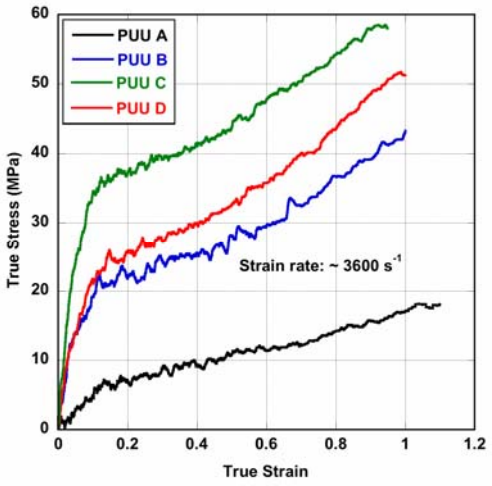

(6B)

Figure 6. A comparison of stress-strain curves for the PUU materials at a low (A) and high strain rate (B)

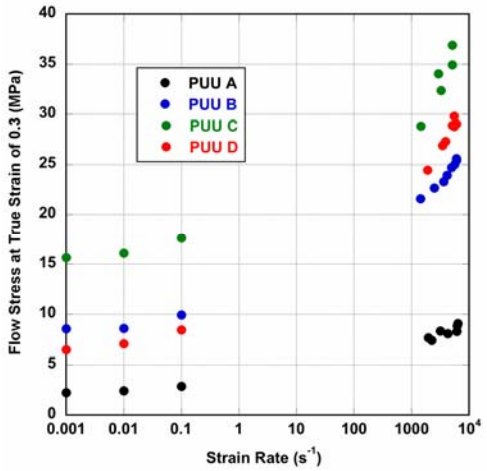

Figure 7. Flow stress values for the PUU materials at low and high strain rates

Stress-strain behavior under uniaxial tension - Figure 8 shows a comparison of the stress-strain curves for the materials under uniaxial tension at a low rate of 10^{-3} /s (note that these tests were terminated prior to the ultimate failure). The stress levels in tension at large strains are significantly greater than those under compression due to increased strain hardening. In tension, the polymeric chains align in an uniaxial direction along the axis of elongation, compared to a biaxial manner in a plane normal to the loading direction under compression. This leads to a greater orientation induced stiffening in tension. Interestingly, at large strains, the curves for the PUU **D** show a greater stiffening than the PUU **B**. This leads to the PUU **D** manifesting lower stress levels at low strains but higher stresses at large strains (notice the crossover of the PUU **D** and PUU **B** curves at 0.85 true strain). The increased phase mixing, which helps increase the rate sensitivity in PUU **D** material, also helps improve its strain hardening behavior.

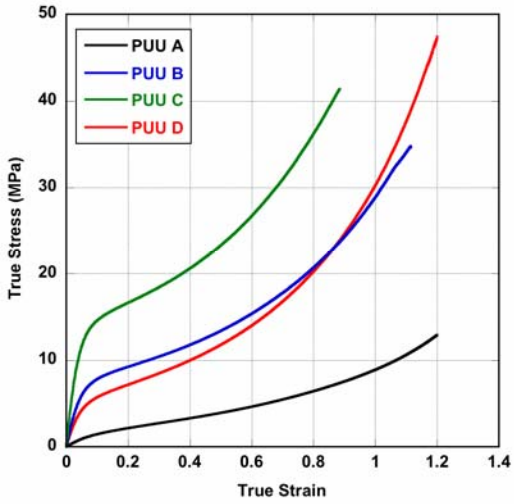

Figure 8. Stress-strain curves under uniaxial tension for the PUU materials

CONCLUSIONS

Mechanical deformation of a select set of model PUU materials was investigated over a broad range of strain rates. Increasing the hard segment content, as expected, increased the stiffness and the flow stress levels. Additionally, altering the SS molecular weight (from 2000 g/mol to 1000 g/mol) was observed to promote phase mixing and increase the intermolecular interactions via hydrogen bonds between the hard and soft segments in the material. This change in material microstructure drastically changed its viscoelastic behavior. Specifically, the nature of its storage modulus curve changed such that it exhibited a greater rise in modulus with decreasing temperature, and its soft segment glass transition temperature displayed a greater rate/frequency dependent

shift. These changes helped greatly improve the rate sensitivity in the material with 1000 g/mol SS MW, such that it showed more compliant behavior at low strain rates, but significantly higher stiffening at high rates. This behavior is highly desirable for a host of applications, where the material is required to possess good flexibility and unfolding capabilities during normal use while also providing improved impact protection. Complementary ballistic tests also confirmed that, among the four model PUU materials, PUU with 1000 g/mol SS MW exhibited the best ballistic performance against impact of .22-caliber fragment simulating projectile.

Furthermore, the increased intermolecular interactions which improved the dynamic strain hardening behavior also helped improve the barrier properties. These findings suggest that tailoring the microstructures and exploiting molecular mechanisms can help enable the design of segmented PUU materials with simultaneous enhancements in both high strain-rate mechanical properties and barrier properties, which is greatly desired for future C/B protective ensembles.

ACKNOWLEDGEMENTS

The authors acknowledge the funding from the U.S. Army to the Institute for Soldier nanotechnologies (ISN) for an FY08 6.2 project. Sai S. Sarva was supported by the ISN through Contract No. DAAD-19-02-D0002 with the U.S. Army Research Office. Alex J. Hsieh also thanks Dr. Rick L. Beyer of Army Research Laboratory for providing assistance with the SAXS and WAXS measurements, and Dr. Shawna M. Liff of ISN for assistance with the tensile tests.

REFERENCES

Abouzahr S, Wilkes GL, Ophir Z. Polymer 1982; 23, 1077-1086.

Chen W, Lu F, Frew DJ, Forrestal MJ. J. of Appl. Mech. 2002; 69, 214–223.

Ferry JD. Viscoelastic Properties of Polymers,3rd ed., New York: John Wiley & Sons; Chapter 11; 1980.

Gray GT III, Blumenthal WR. ASM Handbook, Mechanical Testing and Evaluation, vol. 8: Materials Park, Ohio: ASM International, 10th ed. 2000; vol. 8, 488–96.

Grove CM, U.S. Army Edgewood Research Development & Engineering Center Tech. Report 1999; ECBC-TR-043.

Holden G, Legge NR, Quirk R, Schroeder HE. Thermoplastic Elastomers, 2nd ed., Cincinnati: Hanser/Gardner; Chapter 2; 1996.

Hsieh AJ, Yin J, Pate BD, Boyce MC. 25th Army Science Conference. 2006; Orlando, FL.

Hsieh AJ, Krogman K. Unpublished data, 2008.

James Korley LT, Pate BD, Thomas EL, Hammond PT. Polymer 2006; 47, 3073-3082.

Kojio K, Nakashima S, Furukawa M. Polymer. 2007; 48, 997-1004.

Mulliken AD, Boyce MC. Int'l J. Solids & Struct. 2006; 43, 1331-56.

O'Sickey MJ, Lawrey BD, Wilkes GL. J. Appl. Poly. Sci. 2002; 84, 229-243.

Qi HJ, Boyce MC. Mech. Mater. 2005; 37(8), 817-839.

Sarva SS, Deschanel S, Boyce MC, Chen W. Polymer Comm. 2007; 48, 2208-13.

Sheth JP, Aneja A, Wilkes GL, Yilgor E, Atilla GE, Yilgor I, Beyer FL. Polymer 2004; 45, 6919-6932.

Yi J, Boyce MC, Lee GF, Balizer E. Polymer 2006; 47, 319-329.